T.R.
ONDOKUZ MAYIS UNIVERSITY
GRADUATE SCHOOL OF SCIENCE

MASTER THESIS

INVESTIGATION OF CO_2 ADSORPTION ON MCM-41 BY MONTE CARLO SIMULATION

MÜCAHİT MALKOÇ

DEPARTMENT OF NANOSCIENCE AND NANOTECHNOLOGY

SAMSUN
2019

THESIS APPROVAL

This master thesis study under the name of "**Investigation of CO_2 Adsoption on MCM-41 by Monte Carlo Simulation**" which is prepared and presented by Mücahit MALKOÇ, is approved as Master Thesis in Nanoscience and Nanotechnology Department at Ondokuz Mayıs University by committee members listed below on 16 / 07 / 2019

Supervisor	Asst. Prof. İbrahim İNANÇ Ondokuz Mayıs University Metallurgical and Materials Engineering Department
Committee Member	Assoc. Prof. Özgür DEMİRCAN Ondokuz Mayıs University Metallurgical and Materials Engineering Department
Committee Member	Asst. Prof. Aydemir Güralp URAL Samsun University Aerospace Engineering Department

Approved in __/__/2019

Prof. Bahtiyar ÖZTÜRK

Institute Manager

ETHICAL STATEMENT

I declare that all the information given in this dissertation is true and absolute which is prepared in conformity with the regulations for Ondokuz Mayıs University Graduate School of Science and thesis writing rules, all the information were referred and kept on the right side of the laws according to scientific ethic during the stage of production of information.

Mücahit MALKOÇ

July 2019

ABSTRACT

Master's Thesis

Investigation of CO_2 Adsorption on MCM-41 by Monte Carlo Simulation

Mücahit MALKOÇ

Ondokuz Mayıs University

Graduate School Of Science

Departmant of Nanoscience and Nanotechnology

Supervisor: Asst. Prof. Dr. İbrahim İNANÇ

Global warming and climate change issues have been frequently raised and discussed with the increase of CO_2 in the atmosphere. In addition to CO_2, other gases released into the atmosphere in the flue gas are known to significantly reduce agricultural production through acid rain in industrial zones. For many industries, in both environmental and economical sense, it is extremely important to provide the adsorption of CO_2 waste gases efficiently in a renewable way and to reach high adsorption capacities at low energy consumption levels. With this study, we will examine the adsorption characteristics of the catalyst Mobile Crystaline Material (MCM-41) and aim to contribute scientifically to minimize the damage of espacially CO_2 gas to the environment and decrease the effect of global warming.

In this thesis, mesoporous MCM-41 structure with different ratios of aminopropyl (AP) will be modelled and the adsorption characteristics of this sorbent for different gases (CO_2, SO_2 and H_2O) will be obtained after a set of simulations. First, we will realize modelling of AP/MCM-41 with different amount of AP loadings. Then partial charges of AP/MCM-41 structure will be obtained more realistically by a quantum mechanical calculation method, Density Functional Theory (DFT). By using partial charges obtained from quantum mechanical calculations, Grand Canonical Monte Carlo (GCMC) simulations were conducted in order to analyze the CO_2 adsoption characteristics of AP/MCM-41 and the effect of SO_2 and H_2O to those characteristics which are not explored in detail and understood fully up to now.

July 2019 - 47 pages

Keywords: MCM-41, Molecular Modeling, CO_2 and SO_2 adsorption, GCMC Simulation, Density Functional Theory

ÖZET

Yüksek Lisans Tezi

MCM-41 Üzerinde CO_2 Emiliminin Monte Carlo Simülasyonu ile Araştırılması

Mücahit MALKOÇ

Ondokuz Mayıs Üniversitesi

Fen Bilimleri Enstitüsü

Nanobilim ve Nanoteknoloji Anabilim Dalı

Danışman: Dr. Öğretim Üyesi İbrahim İNANÇ

Son zamanlarda atmosferdeki CO_2 oranının artmasıyla birlikte küresel ısınma ve iklim değişikliği konuları sıkça gündeme gelmekte ve tartışma konusu olmaktadır. CO_2'in yanında baca gazı içinde atmosfere salınan diğer gazların, sanayi bölgelerinde asit yağmurları yoluyla tarımsal üretimi önemli ölçüde azalttığı bilinmektedir. Bu yüzden birçok sanayi alanında meydana gelen özellikle CO_2 gibi atık gazların emiliminin sağlanması, düşük enerji tüketimlerinde yüksek emilim kapasitesine nasıl ulaşılabileceği ve yenilenebilirliğinin nasıl sağlanabileceği konuları hem çevresel hem de ekonomik anlamda son derece önem arz etmektedir. Bu çalışmada büyük endüstriyel fabrika bacalarından çıkan, çevreye zararlı ve küresel ısınmaya sebep olan, özellikle CO_2 gazının emilimini gerçekleştirecek Mobil Kristal Malzeme (MCM-41) katalizörünün emilim karakteristiklerini çalışarak bilim ve endüstri dünyasına bu gazların çevreye verdiği zararı en aza indirme konusunda katkı sağlanması amaçlanmıştır.

Bu tez çalışmasında, farklı oranlarda aminopropil (AP) içeren gözenekli MCM-41 yapısı modellenmiş ve bu sorbentin farklı gazlar (CO_2, SO_2 ve H_2O) için emilim özellikleri bir dizi simülasyondan sonra elde edilmiştir. Öncelikle, AP / MCM-41'in farklı AP yükleri modellemesini gerçekleştirdik. Daha sonra, kuantum mekaniksel hesaplama yöntemi olan Density Functional Theory (DFT) ile daha gerçekçi sonuç elde etmek için AP/MCM-41'in kısmi yükleri elde edildi. Kuantum mekanik hesaplamalardan elde edilen kısmi yükler kullanılarak, AP/MCM-41'in CO_2 tutma özelliklerini ve CO_2 emilim özelliklerine SO_2, N_2ve H_2O'nun etkilerini analiz etmek için Grand Canonical Monte Carlo (GCMC) simülasyonları yapılmıştır.

Temmuz 2019 - 47 sayfa

Anahtar kelimeler: MCM-41, Moleküler Modelleme, CO_2 ve SO_2 Emilimi, GCMC Simülasyonu, DFT

ACKNOWLEDGEMENTS

I would first like to thank my thesis advisor Asst. Prof. İbrahim İNANÇ of the Nanoscience and Nanotechnology Department at Ondokuz Mayıs University. The door to Asst. Prof. İbrahim İNANÇ office was always open whenever I ran into a trouble spot or had a question about my research or writing. He consistently allowed this thesis to be my own work but steered me in the right direction whenever he thought I needed it.

Also, I am gratefully indebted to master student Ahmed ALSHAER for his very valuable contributions at the stage of simulation.

Finally, I must express my very profound gratitude to my parents and to my family for providing me with unfailing support and continuous incentive throughout my years of study and through the process of researching and writing this thesis. This accomplishment would not have been possible without them.

Thank you.

Author

Mücahit MALKOÇ

CONTENTS

ABSTRACT iii
ÖZET iv
ACKNOWLEDGEMENTS v
CONTENTS vi
LIST OF SYMBOLS AND ABBREVIATIONS vii
FIGURES viii
TABLES ix
1. INTRODUCTION 1
1.1. M41S Family 2
1.1.1. MCM-41 Materials 3
1.2. Aim of This Study 4
1.3. Advantages and Disadvantages of MCM-41 5
1.4. Why MCM-41? 6
1.5. Synthesis of Mesoporous Silica MCM-41 6
1.6. Application Area of MCM-41 7
1.7. Why Simulation? 7
1.7.1. RASPA: Molecular simulation software 8
1.7.2. Materials Studio Program 9
1.7.3. Introduction of Monte Carlo simulation method 10
1.7.4. Grand Canonical Monte Carlo (GCMC) simulation 12
1.7.5. GCMC simulation model of carbon dioxide adsorption 13
2. LITERATURE RESEARCHES 15
3. SIMULATION METHOD 18
3.1. Modeling of AP/MCM-41. 18
3.2. Computational Method and Parameters 19
3.3. Quantum Mechanical Modeling 20
3.4. Surface Area Calculation 22
3.5. Reaction Mechanism 22
3.6. GCMC (Grand Canonical Monte Carlo) Simulation 22
3.6.1. AP concentration effect 222
3.6.2. Effect of N_2 to CO_2 adsorption calculations 23
3.6.3. The impact of H_2O to CO_2 and SO_2 adsorption processes 24
4. RESULTS AND DISCUSSION 24
4.1. Effect of AP Concentration to CO_2 Adsorption 24
4.2. Effect of Flue Gas N_2 on CO_2 Adsorption 25
4.3. Atomic Partial Charges of Aminopropil+SiO_2 26
4.4. Effect of H_2O on CO_2 Adsorption 27
4.5. Effect of SO_2 on CO_2 Adsorption 28
4.6. Effect of Temperature on CO_2 Adsorption 29
5. CONCLUSIONS 30
6. REFERENCES 311

LIST OF SYMBOLS AND ABBREVIATIONS

AP/MCM-41	Aminopropyl/Mobil Composition Material No:41
APTMS	Aminopropyltrimethoxysilane
CBMC	Configuration Biased Monte Carlo
CFCMC	Continuous Fractional Component Monte Carlo
DFT	Density Function Theory
GCMC	Grand Canonical Monte Carlo
HOMO	High Occupied Molecular Orbital
IAST	Ideal Adsorbed Solution Theory
IPCC	Intergovernmental Panel on Climate Change
IUPAC	International Association of Pure and Applied Chemistry
KMC	Kinetic Monte Carlo
LUMO	Low Unoccupied Molecular Orbital
M41-S	Family of MCM-41, MCM-48, MCM-50
MC	Monte Carlo
MCM-41	Mobil Composition Material No:41
MD	Molecular Dynamics
MOF	Metal Organic Framework
PEI	Polyethylenimine
PSD	Pore Size Distribution
TEOS	Tetraethylorthosilicate
TMOS	Tetramethylorthosilicate

FIGURES

Figure 1.1. The schematic representation of MCM-41, MCM-48, MCM-50……2

Figure 1.2. The schematic representation of MCM-41(a), Two dimensional hexagonal pore structure of MCM-41(b)…….....3

Figure 1.3. Prosess of Synthesis of MCM-41……...…….……....7

Figure 1.4. Adsorption of arbon dioxide densities for selected slit pores and temperatures…….……14

Figure 3.1. Modeling of MCM-41 with different AP loadings …..…...….....19

Figure 3.2. Interaction potentials to be used in geometricoptimization and GCMC..20

Figure 3.3. Representing Connolly, Accessible and Van der Waals surface area..…...21

Figure 3.4. Sequence of reactions performed by AP/MCM-41 with CO_2……...22

Figure 3.5. AP2, AP4, AP8 Connolly Surface area of simulation picture on Materials Studio program…….23

Figure 4.1. Adsorption isotherm curves of different AP loading on MCM-41……..24

Figure 4.2. Adsorption isotherm curves of AP/MCM-41 with CO_2 (100%) and CO_2+N_2 (75%+25%).....25

Figure 4.3. Adsorption isotherm curves of AP/MCM-41 with CO_2 (100%) and CO_2+N_2 (100%+25%)……..25

Figure 4.4. Adsorption isotherm of CO_2 adsorption with H_2O (1%, 2%, 3%) on AP/MCM-41……...……...……...……27

Figure 4.5. Adsorption energy values of CO_2 at different H_2O loading (1%, 2%, 3%)……..…….27

Figure 4.6. Adsorption isotherm of CO_2 with SO_2 (0.1%, 1 %, 10 %) on AP/MCM/41…….28

Figure 4.7. Adsorption energy values of CO_2 at different SO_2 loading (0.1%, 1%, 10%)…….28

Figure 4.8. Comparison of Temperature effect of CO_2 adsorption on AP/MCM-4...29

Figure 4.9. Adsorption energy values of CO_2 adsorption at different temperature (298K, 348K, 398K) on AP/MCM-41…..…….……..….29

TABLES

Table 1. Structural properties of the AP/MCM-41 model……..20
Table 2. Comparison of atomic partial charges by different method ...……27
Table 3. Comparison between Amines group atomic partial charges …..……28

1. INTRODUCTION

In the last 40 years, synthesis, characterization and property assessment of porous materials and molecular sieves for catalysis, adsorption, separation and environmantal pollution control processes have been studied (Zhao, 1996). Due to the demands of industrial and basic studies, there has been an increasing interest in the expansion of pore sizes from micro pore to mesopore region. Separation of heavy metal ions, separation of large organic molecules from waste water and selective adsorption, formation of supramolecular assembly of molecular sequences, encapsulation of metal complexes in frames and introduction of nanometer particles for electronic and optical applications are examples of needing larger porous than micro porous. As a result of these demands, a significant amount of work was carried out to create porous materials with larger pore diameters than conventional nanoporous (Alothman, 2012).

In 1992, Mobile Oil Corporation scientists, the M41-S family (Melo, 1999). A new family of molecular sieves synthesized. This type of sequential mesoporous materials consists of MCM-41, MCM-48 and MCM-50 (Hoffmann, 2006). MCM-41 has attracted the interest of scientists as it has high surface area, high thermal and hydrothermal stability, controllable pore size, hydrophobicity and acidity. This porous material consists of hexagonal channels with diameters ranging from 1.5 to 10 nm. These properties of this material make it a promising catalyst and support material and can be used in the industry for adsorption, ion exchange and Environmental Control (Melo, 1999).

MCM-41 received great attention in the field of separation and adsorption. The single type pore structure and high pore volume in the mesopore range make the MCM-41 available for different separations from the removal of organic and inorganic contaminants. MCM-41 has been characterized by adsorption of various molecules such as carbon dioxide, nitrogen, oxygen, water, cyclopentane, toluene and carbon tetrachloride and alcohols (Selvam, 2001; Vartuli, 2001). These early studies showed remarkable high adsorption capacity of MCM-41 for hydrocarbons like benzene compared to conventional micro-porous molecular sieves (Vartuli, 1998).

1.1. M41S Family

Porous silica materials made of self-assembled surface active agents as templates have attracted considerable attention in recent years. The family of high-grade meso silica materials called M41S (MCM-41, MCM-48 and MCM-50) are known as new potential molecular sieves and supportive materials (Kresge, 1992; Beck, 1992). In parallel with the development of M41S materials, several other sequential mesophases with similar properties have been synthesized. A lot of studies have approved successful applications of these semi-crystalline silica zeolites. Meso silicas conjugated to functional active groups or transition metals have shown to have selective separation and catalytic activities due to the fact that the porous network facilitates transferring mass of reactants to the active sites (Tanev, 1994).

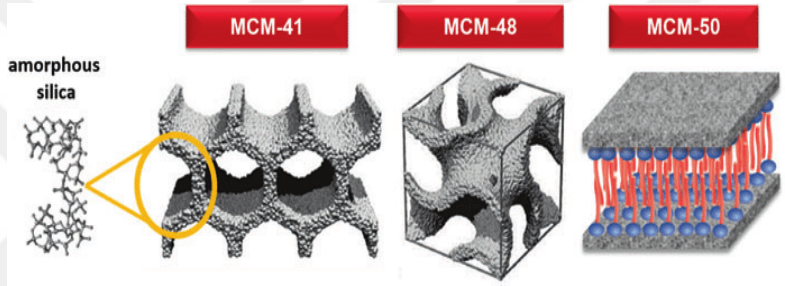

Figure 1.1 The schematic representation of MCM-41, MCM-48, MCM-50 (Schwanke et al. 2017)

Impotant discovery of MCM-41 materials by researchers at Mobil in 1992 has led to research on enzymes, membranes, sensors as separations, selective adsorption, fixed phases in chromatography, pre-concentration of trace metals, heterogeneous catalysis, biochemistry and biological applications (immobilization, recognition, drug distribution, etc.) irradiated materials for nuclear waste heavy metals, laser and optical device applications, and controlled polymerization in pores (Moller and Bein, 1998; Diaz and Balkus, 1996; Xu et al., 2003; Llewellyn et al., 1994). The existance of big and adjustable uniform pores makes it possible to shape selective transformations of bulk molecules and pharmaceutical (Corma, 1994). In addition, it can find other potential applications such as surface modified porous molecular sieves, gas and separations by liquid chromatographic. Different methods for this final application have been assessed to synthesize mesoporous silica particles with spherical shapes and narrow pore size distribution (Raimondo, et al., 1997; Grün, 1996; Sierra, 2000).

Generally, the formation process of meso-structured silica is to use surfactants as building agents. Organosilicate compound such as tetramethylorthosilicate

(TMOS) or tetraethylorthosilicate (TEOS) are used as silica source. These silicic acid tetraesters, which are very easily polymerized and not isolated at all, can be considered as $Si(OH)_4$. They are insoluble in water, but could be dissolved in a mixture of water and a water-miscible organic solvents. When the pH is lowered or increased, they are hydrolyzed, the ester bond separates to produce an alcohol and free silanol group. Silanol group is a reactive and undergoes series of condensation reactions with other silanol groups. According to the presence of pH and salts, condensation can contributes to particle growth gelatation through relatively well understood processes (Berggren, 2005). The resulting structure is affected by a number of parameters: precursor selection, surfactant selection, presence of specific ions, condensation rate, mainly pH and temperature. A low reaction rate appears to promote the formation of a fine-arranged crystalline material. For example, single crystalline crystals of monoporous materials with cubic geometry were obtained by runing the reaction at 273 K; in this case a less ordered product was obtained (Sakamoto, 2000). It is possible that the control of the crystal morphology, which can be achieved with low temperature, proceeds under thermodynamically controlled conditions, which is not always the case (Che, 2001).

1.1.1. MCM-41 Materials

MCM-41 is used as a member of the M41-S family because the other members are thermally unstable (MCM-50) or difficult to obtain (MCM-48). It also stands out for its high surface area, high thermal and hydrothermal stability, controllable pore size, hydrophobicity and acidity.

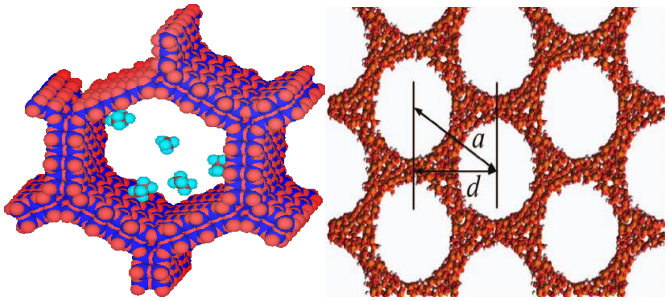

(a) (b)

Figure 1.2. The schematic representation of MCM-41(a), Two dimensional hexagonal pore structure of MCM-41(b) (Bristol, 2010)

As shown in Figure 1.2, the structure of the MCM-41 type mesopous materials is unmatched, unidirectional and similar to the honeycomb structure. The internal

surface area is about 1000 m^2/g and the hexagonal arranged channel diameters range from 1.5 to 10 nm.

The pore surface of the MCM-41 is heterogeneous due to the hexagonal shape of the pore visible in the figure above. Siloxane bridges developed at the corners of the pores. These bridges help to form hydrophobic portions on the pore surface. On the other hand, the flat areas of the pore surface are hydrophilic due to hydroxyl groups.

The formation mechanism of MCM-41 draws more attention to research. As a result of studies on formation mechanism, two mechanisms have been proposed. One of these mechanisms, Beck et al., the proposed mechanism is the liquid crystal template (LCT). Other formation mechanism Stucky et al., the mechanism of conversion from lamellar to hexagonal phase.

1.2. Aim of This Study

Nowadays, it is known in the scientific community that the main cause of global warming is the increase in the amount of carbon dioxide. Physical containment and storage of CO_2, it is seen as a rapidly rising option in recent years that the struggle with climate change and the reduction of the effects of climate change. Especially with the increase in the proportion of flue gases, CO_2 and SO_2, global warming and climate change issues have often been a subject of debate.

Our initial goal is to obtain a model of the aminopropyl (AP)-functional MCM-41 structure for different pore sizes. This model will be doped by different amounts of AP loads of MCM-41 structure obtained from previous studies and optimum AP loading amount will be determined. The structure of the AP/MCM-41 at different concentrations created will be geometrically optimized with the Materials Studio (MS) program and the force field parameters will be obtained from MS database. With the aid of the NWChem program, which is free and multi-processor operation feature, partial loadings will be found by quantum mechanical calculation by studying different AP reaction sequences obtained from experimental results. In order to investigate AP/MCM-41 in more detail, the effects of different AP loads, SO_2 concentration and moisture content on CO_2 adsorption characteristics at different temperatures and pressures using the Grand Canonical Monte Carlo (GCMC) simulation technique are obtained at the molecular level and compared with the experimental results.

1.3. Advantages and Disadvantages of MCM-41

Mesoporous materials initially appeared as sacred bowls sought by zeolite chemists of the time. They have generally high surface areas and are easily accessible, with regular pores and regular arrays. Significantly, pore sizes are higher than those could achieved in zeolites and can sometimes be adjusted in the nanometer range (1.5-10 nm) by selecting a suitable surfactant-paced system with an auxiliary solvent or swelling agent. They have relatively thin walls that prevent secondary pores from entering the walls, forming only fine particles and having low hydroxyl groups (Stein, 2000).

The pores of sequenced silicate mesoporous materials to be used in separation applications consists of a series of normal pores, controllable pore size and the ability to functionalize the surface for specific separations (Kisler at al., 2003). Potential separation applications for MCM-41 include mercury separation from waste streams (Mercier and Pinnavaia, 1997; Feng, 1997). However, the stability of these materials in aqueous solutions is of concern. Although the properties of M41S materials have been widely investigated, only limited studies have been performed after their exposure to aqueous solutions. Most of these studies have focused on the hydrothermal stability of the materials by assessing their structure before and after treatment in boiling water for up to 48 h (Lim and Stein, 1999; Yamamoto and Tatsumi, 2001). But, if these materials are supposed to be used in separation processes economically involving aqueous solutions, it is vital to maintain integrity of the pore structure over repeated cycles of adsorption and regeneration (usually carried out at room temperature).

Recent studies have shown that M41-S materials have been modified by long exposure to water and water vapor; this leads to a reduction in structural regularity, pore shape homogeneity, pore size and pore volume. (Ribeiro, 1999; Zhao, 1998; Igarashi, 1999). In particular, the base solutions lead to a greater loss of structure with a much larger porosity and cause a reduction in surface areas found in materials that have been immersed in water for a short time, for example, few hours. (Landau, 1998; Trong, 1998). It was found that immersion in water had a greater effect on the structure as the solution temperature increased in the range of 298-373 K. This low stability limits the life of the M41S materials in aqueous solutions and limits the range of application for these materials.

Gusev et al. stated experimental data on the mechanical stability of the silica mesoporous material MCM-41. By applying X-ray diffraction and nitrogen adsorption, they concluded that the ordered mesoporous structure of MCM-41 can be mainly influenced by mechanical compression at pressures as low as 850 atmospheres and basically destroyed in 2200 atmospheres (Gusev, 1996).

1.4. Why MCM-41?

The main purpose of using carrier materials in CO_2 capture and storage, to provide a large surface area and to improve the physical and mechanical properties of the sorbent. Recently academic and industrial research has promising greater hopes of solid sorbents at CO_2 capture. Moreover; well defined pore shape (hexagonal/cylindrical), quite regular pore alignment, pore size adjustable, large pore volume and consequently high adsorption capacity, high surface area, good surface reactivity, easy to change surface properties, catalytic properties can be improved depending on the desired reaction, due to the high thermal, hydrothermal, chemical and mechanical stability, MCM-41 material is more forefront than other carrier materials.

1.5. Synthesis of Mesoporous Silica MCM-41

The synthesis of mesoporous materials is one of the of the mainly issues in modern medicine science. Since the discovery of the M41-S porous molecular sieve family in Mobile Oil Corporation, synthesis and applications of porous materials prepared as templates are of perfect interest. Basic properties of MCM-41 materials high thermal stability, wide surface area and narrow pore size distribution.

Different synthesis strategies were successful and proposed, some reported synthesis for mesoporous MCM-41. However, all these operations have a common aspect besides the apparent presence of a material source in the template, which is silica. A template is a structural orientation agent, generally a relatively simple molecule or ion, where a frame is created. The favorite patterns for MCM-41 synthesis are quaternary ammonium ions with a long alkyl chain, usually a hexadecyl group.

Once MCM-41 is formed, the pores are filled with the templates and the micelles must be removed to obtain a fully porous support material. The most elegant solution to this demand is to remove the template repeatedly by washing it with mixtures of

(slightly acidified) organic solvent and water, resulting in the removal of the stencil. The resulting solutions that contain the template are evaporated to recover the template. If the synthesis conditions are relatively moderate, the template does not decompose and can be reused for the next synthesis.

The most common applied template for MCM-41 synthesis is a setyl trimethyl ammonium bromide (or chloride), that is, an alkyl chain containing sixteen -CH_2 moieties. This template synthesize MCM-41 uniform pore size. The MCM-41 pore size is under effect of using longer or shorter alkyl-chain templates (Figure 1.3).

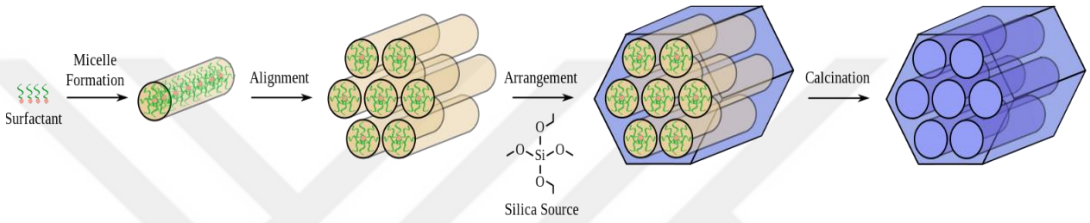

Figure 1.3. Prosess of Synthesis of MCM-41 (Wikipedia, 2019)

1.6. Application Area of MCM-41

MCM-41 type catalysts in their own (in pure silicate form); at the adsorption of environmental health threatening compounds such as benzene, carbon dioxide and methane, in wastewater treatment, in pharmaceutical and medical applications, and they are used in membrane production, etc.

At the same time, elements and compounds such as metal, metal oxide or heteropoly acid are added to the structure to increase the catalytic activity. So, catalysts that increased activity by this method; oxidation, hydrogenation, etherification, esterification and isomerization they can also be used with high selectivity value in many different reactions.

1.7. Why Simulation?

Despite of many experimental studies in this area, the effects and interactions of amines on amorphous surfaces are not fully understood. In recent years, in addition to these studies, modeling and simulation studies at the molecular level have been used to gain a new perspective. In this study, we will use quantum mechanical and Monte

Carlo simulation methods to contribute to the study in this field. We will perform our simulations with Materials Studio program and different open source code RASPA and NWChem softwares.

1.7.1. RASPA: Molecular simulation software

Molecular sieves are selective, high capacity adsorbents due to their high intracrystalline surface areas and strong interactions with adsorbates. Molecules of different sizes generally have different diffusion properties in a given molecular sieve, and the molecules can be separated according to their size and structure according to the size and geometry of the sieve holes. A lot of progress has been made in understanding the subtle interaction between molecules and restriction, and most of this understanding comes from computer simulations that can analyze chemistry and physics at an atomic level.

Two main computational approaches to overcome these systems are: (I) quantum mechanical calculations and (ii) force field-based simulations. The first approach is needed to examine properties such as bond breaking and formation, and is available in many excellent commercial and non-commercial packaging. The second approach is useful for studying larger systems and calculating a wide variety of thermodynamic and dynamic properties. Power domain approaches include Monte Carlo (MC) simulations, molecular dynamics (MD) simulations, and energy reductions. In this study we used RASPA, a code that focuses on minimizing systems described by MC, MD and conventional force fields.

The RASPA code was written as a collaboration between Northwestern University (USA), University of Amsterdam (Netherlands) and University Pablo de Olavide (Spain) and has recently contributed to the University of Delft (Netherlands). The code was originally based on the object-oriented Fortran 90 (Al., 2003; Chempath, 2013) of the Snurr group from David Dubbeldam's postdoctoral project (2006–2009) at Northwest University.

RASPA is a serial code. For a simple system, a single isotherm point can be obtained within hours and for days for more complex systems. MC codes are ideal for task farm parallelism. Here, the simulations are independent and include temperature, pressure, etc. As different as the series is run as simulation sets. For example,

(assuming there is no hysteresis), each point of an isotherm can be operated independently. The memory requirements of MC codes are modest.

Programs can be written in a variety of ways, but it is often true that the fastest code is probably the most difficult to read, but certainly legibility-based programs are inactive. RASPA (being a 'research' code) selects the middle foundation and is based on the following ideas:

- Correctness and accuracy. For all the techniques and algorithms available in RASPA, we have implemented the “best” in the literature (in our opinion). For example, RASPA configuration uses biased Monte-Carlo (CBMC) and continuous fractional component Monte Carlo (CFCMC); uses Ewald sum for electrostatic, MD relies on sympathetic and precautionary integrators.
- Check-in is easy. The requirements of the input files are kept as small as possible. Additional commands in the input file are required only for more advanced options. Also the input format is simple. Leakage coefficients and excess adsorption are calculated automatically.
- An integrated simulation environment. The code consists of many functions and routines that can be easily combined. MD can be used in MC and vice versa. Code is relatively easy to expand and modify.

1.7.2. Materials Studio Program

Materials Studio is software that proposes a wide range of features to model materials. The Material Viewer provides basic modeling capabilities and software infrastructure.

There are separate products that integrate into Materials Studio to create a comprehensive range of materials modeling tools:

- Amorphous Cell - Model construction and property prediction for non-crystalline materials, particularly polymers, organic liquids, and their mixtures.
- CASTEP - First-principles plane-wave pseudopotential code for quantum mechanics-based simulation of solid-state materials.
- Forcite - A collection of molecular mechanics tools that allow you to investigate a wide range of systems, in which the key approximation is that the potential energy surface on which the atomic nuclei move is represented by a classical forcefield.

- Gaussian Interface - A tool that gives access to the popular Gaussian application which employs Hartree-Fock and density functional theory methods to study molecular systems, allowing prediction of structural, thermodynamic, and electronic properties, and NMR and vibrational spectra.
- Sorption - A tool that allows you to simulate a sorbate absorbed in a sorbent framework in order to calculate properties such as adsorption isotherms, binding sites and energies, density and energy fields, energy distributions, isosteric heats, and Henry constants.

1.7.3. Introduction of Monte Carlo simulation method

Monte Carlo techniques that can be used to calculate equilibrium properties of classical multi-mass systems. In this subject, the word "classic means compliance with the classical mechanical laws of the core motion of the constituent particles. This is the perfect approach for a wide range of materials. But when we consider the translational or rotational motion of light atoms or molecules (He, H_2, D_2) or the vibration motion with a frequency such as $hv>k_BT$, we should be carefull about quantum effects.

Before I begin to explain the MC method, in brief, I have to explain the role of computer simulations in general. This subject is discussed considering the situation before the emergence of the best electronic computers. At that time, there was only one way to predict the outcome of an experiment, namely, using a theory that provides an approximate definition of the system being studied. Almost always, a theory is used because there are very few model systems in which balance properties can be fully calculated (examples are ideal gas, harmonic crystal, and a series of two-dimensional lattice models). As a result, most properties of real materials have been estimated based on approximate theories.

Given enough information about inter-molecule interactions, these theories will provide us with an estimate of the characteristics of interest. Unfortunately, our knowledge of all intermolecular interactions is very limited except for the simplest molecules. If we want to test the validity of a particular theory by directly comparing it with the experiment, this leads to a problem. If we find that this theory and experiment are incompatible, it may mean that our theory is wrong, or we have made a wrong assumption about inter-molecular interactions or both. A particular model system, without having to rely on approximate theories. On the other hand, we can

compare the result of a particular model system simulation with the approximate analytical theory estimates applied to the same model. Now, if we find that this theory and simulation are incompatible, we know that theory is wrong. Therefore, in this case, computer simulation is designed to test the design theory of the experiment. This method is called a "computer experiment" to "scan" the theories before applying them to the real world. Computer experiments have become a standard practice as they perform the first (and usually last) test of a new theoretical result.

In fact, the first date of computer simulation shows the role of computer simulation. In some areas of physics, there was little need for simulation because there were very good analytical theories (for example, to predict the properties of dilute gases or almost harmonic crystal solids). However, in other areas, if there is any “definite” theoretical result, very few were known and progress was prevented much from the fact that there was not a precise test to assess the quality of the theory. The situation here is intensive fluid theory (Metropolis, 1953).

This could explain why in the 1950s, the first time electronic computers were introduced for unclassified research, the numerical simulation of condensed liquids was one of the first problems addressed. In fact, the first simulation of a "liquid" was the Metropolis et al. In Los Alamos, using the Monte Carlo method (or to identify it more accurately). At almost the same time, Fermi, Macaroni and Ulam, unharmonic, conducted a very famous numerical study of the dynamics of a one-dimensional crystalline. However, the first appropriate molecular dynamic simulations were reported by Alder and Wainwright at Livermore in 1956, which examined the mounting dynamics of solid spheres. The first MD simulation of a model for a "real" material was simulated by the Bond group in Brookhaven in 1959 (and published in 1960), for a historical account of radiation damage to the crystal Cu. The first MD simulation of a real liquid (argon) was reported by Rahman in Argonne in 1964. After that, computers were increasingly introduced to scientists outside the U.S. government labs and simulation applications began to spread across other continents. Many of the methodologies of MD simulations have been developed since then, but it is fair to say that basic algorithms for MC and MD have been difficult to change since the fifties.

1.7.4. Grand Canonical Monte Carlo (GCMC) simulation

The most common simulation methods for molecular systems are Monte Carlo and Molecular Dynamics. These methods provide a link between microscopic (molecular level) and macroscopic behavior by evaluating the basic equations of statistical mechanics. The most important advantage is that they can treat large systems with a large number of molecules in relatively short time.

The first theoretical studies aimed to investigate gas adsorption in porous solids were published in the 1960s (Alder and Wainwright, 1960). Nowadays, gas adsorption is considered to be an extremely useful tool for describing computer simulation and also analyzing experimental results to predict gas solid balances.

Various industrial (food, pharmaceutical and petrochemical industries) and geophysical applications for adsorption, pollution control and environmental protection, mixture separation, water treatment and gas storage in porous materials (Ruthven, 1984). In addition, gas adsorption measurements are widely used in materials science as a reliable method to characterize porous materials (Gregg and Sing, 1982; Lowell and Shields, 1991).

Porous materials are catagorized by the International Association of Pure and Applied Chemistry (IUPAC) as macroporous with less pore diameter than 2 nm, 2 to 50 nm pore width and larger pore diameter than 50 nm (Everett, 1972). The pore width is defined as the distance between the diameters D in cylindrical pore or opposite walls in slit pore. Modern industrial and technological needs have led to the development of new materials with extremely small porosity (and vice versa). The size of these pores approaches several molecular anchors, and these pore systems and materials produce a vast range of properties that are completely different from mesopores and large micropores. Adsorption is perform based on the structural properties of the adsorb material, e.g. specific surface area, porosity and pore size. In general, the presence of a large specific surface area and a plurality of easily accessible small-size pores, the desired adsorbent area, as with the pores of molecular dimensions, is further densified by the overlapping solid wall potentials, resulting in increased adsorption capacity.

The pore filling mechanism is described for mesopores and macropores. The Kelvin equation is a thermodynamic model that uses relative pressure (P/P_0) where the capillary is applied at subcritical temperatures. Pore width condensation occurs (Gregg

and Sing, 1982). DFT is less-dependant on computations and can contribute to accurate explanation as working with simple liquids (spherical molecules) and simple geometries. However, MC is defined as an appropriate alternative approach because microscopic models sensitivity is primarily based on the correct representation of molecules, including partial charges and atomic regions (Samios et al., 1997; Samios et al., 2000).

This method is applicable for carbon materials containing a large number of studies on adsorption of different gases. For example, over the past decade, adsorption of porous solids can provide a useful tool for solving the difficult environmental problem of high CO_2 atmospheric concentrations. Activities include CO_2 separation, collection and, finally, storage in geological formations (such as oil and gas fields, coal deposits and salt water). Therefore, in closed areas such as nanaopores, the behavior of CO_2 molecules during adsorption is very important. Gas adsorption, on the contrary is totaly used for characterization of porous carbon in terms of pore size distribution (PSD). The method is made up of experimental and simulated adsorption isotherms such as N_2, CO_2, Ar and more recently H_2 (or combinations thereof) to calculate the optimal distribution of pore sizes of a material (Samios et al., 2000).

1.7.5. GCMC simulation model of carbon dioxide adsorption

Nanopores carbon dioxide shows many differences in hydrogen adsorption. The main reason for this is that although H_2 is critical at 77K, the critical carbon dioxide temperature is 31.25 ° C (304.4 K) and is too high to liquefy even at room temperature. The shape of isotherms gradually changes and causes capillary condensation at pressures far below the vapor pressure. The final shape of the condensation pressure and consequently the adsorption isotherm is determined by the interaction of the fluid and the fluid solids with the pore size and geometry. In this context, the carbon dioxide adsorption isotherms in slit-shaped and cylindrical pore models were calculated using the GCMC method.

The carbon dioxide isotherms obtained by the GCMC simulations for typical slit-shaped pores of selected sizes (*H* up to 2.0 nm) and temperatures are presented in Figure 1.4. Detailed pertinent work is reported elsewhere (195.5 and 308K: Samios et al., 1997; Samios et al., 2000, 253 and 298 K: Konstantakou et al., 2007a, Konstantakou et al., 2007b, 195.5, 253 and 273 K: Konstantakou et al., 2010). As

expected, higher adsorption capacities are observed as temperature decreases. The adsorption mechanism can be divided into three zones: initially small pressures, micro molecules consist of gas molecules covering all the free space adjacent to the walls, fill and adsorption are almost completely controlled by solid-liquid interactions; high pressure, relatively weak in interaction, and larger pores are derived from the reduced isotherm inclination developed in physics multi-layer.

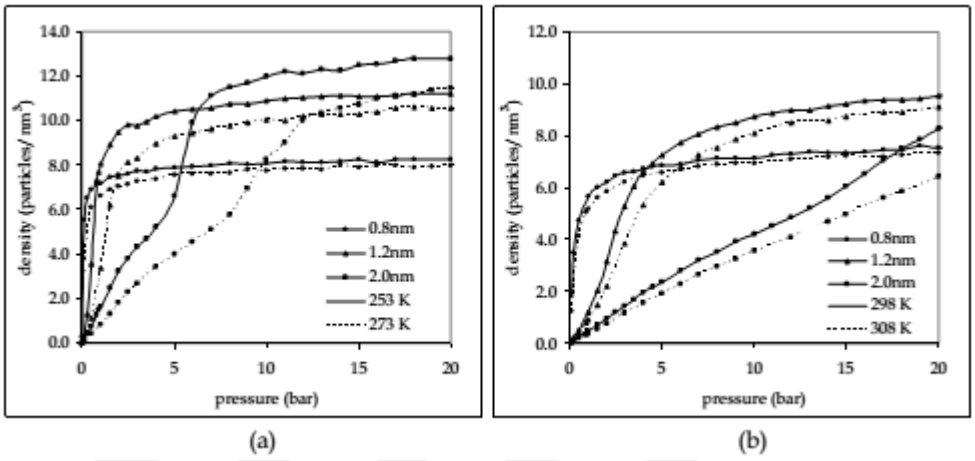

Figure 1.4. Adsorption of carbon dioxide densities for selected slit pores and temperatures (Konstantakou et al., 2011)

In general, the gas-liquid phase transition in pores (capillary condensation) is a very interesting feature observed when condensation gases are held in small cavities. This phenomenon has been extensively studied in both experimental and theoretical terms on the pores of various geometries (Evans and Tarazona, 1984; Ravikovitch et al., 2001; Nilson, 1999; Neimark et al., 2003). In addition, a hysteresis cycle occurs frequently, starting from such filled pores and decreasing the pressure (desorption), and evaporation occurs at lower pressures than observed for condensation. When large pores are connected, the types of rings are observed, especially for very small pore sizes, depending on the shape and relative size of the pores, condensation-evaporation steps can almost completely be reversed. In the hysteresis cycle, GCMC does not adequately define the presence of gas-liquid coexistance (Panagiotopoulos, 1987; Mcgrother and Gubbins, 1999; Neimark and Vishnyakov, 2005).

2. LITERATURE REVIEW

In many experimental and few simulation studies on the CO_2 adsorption of AP/MCM-41, the effects and interactions of AP functional groups on the sorbent surface are not fully understood.

Schumacher et al. simulated CO_2 adsorption on amine functionalized phenyl groups on MCM-41 using the co-condensation method. The same workgroup used GCMC simulation technique to form organic groups that are directly attached to silica atoms of MCM-41.

A similar approach to Williams et al. have studied on MCM-41 by injecting different organic groups. In subsequent studies they used the same unit cells and functionalized materials. Williams et al. observed that the simulations were similar to those after the functionalization.

Zhuo formed four porous hexagonal MCM-41 model, studied the CO_2 adsorption on MCM-41 using the GCMC and Kinetic Monte Carlo (KMC) simulation methods.

Liu and Seaton simulated CO_2 adsorption by grafing groups of amines in different numbers and types onto MCM-41 and tried to understand the interaction between the amine groups and CO_2 by GCMC.

Wang et al. simulated isoterm curves of CO_2 adsorption on MCM-41 and matched this model with experimental results. The CO_2 distribution in MCM-41 channels was studied by MD simulation method and the energy distribution histograms of CO_2 adsorption peak curves of MCM-41 were discussed. The effect of polyethylenimine (PEI) charges on CO_2 adsorption peaks, working capacities and isothermal temperatures were investigated in more detail using the GCMC simulation method.

Maddox and Gubbins used a one-dimensional model to investigate the adsorption of Ar and N_2 in MCM-41 and buckytube in Monte Carlo simulation. A disadvantage of the multidimensional potential model is that the solid-liquid potential and the density of the liquid only change in normal direction to the pore wall and the formation of a strong layer in the adsorbed phase. As an improvement, Maddox and Gubbins developed a two-dimensional potential model which is dependent on radial

and axial directions. In their simulation work, the skeleton of MCM-41 were composed of randomly distributed O atoms and divided into eight section. Each section exerted individual interaction with fluid molecules.

Yun et al. using the ideal adsorbed solution theory (IAST) and GCMC simulation, predicted MCM-41 adsorption capacity with a single-layer cylinder wall model.

He, Seaton and Koh et al. were studied adsorption simulations based on three types of models: (1) a cylindrical Wall model with almost homogeneous pore surface; (2) a quartz normal model with heterogeneous but still normal surface and (3) an amorphous silica model with heterogeneous irregular surface. The amorphous silica model is widely used by engraving cylindrical pores from an amorphous silica matrix.

Feuston and Higgins made a systematic study of the structural influence of different caving pore sizes and wall thicknesses by using molecular dynamics method.

Coasne et al. made a very significant contribution to discover MCM-41, MCM-48, SBA-15 3D-connected topological models from amorphous silica skeletons and revealed the adsorption behaviors of capillary condensation.

Ho et al. completed a hybrid MCM-41 model from an amorphous silica matrix coated physical solvents to interpret the CO_2 solubility behavior. KMC model, Schumacher et al. it is built with the most complex and complex MCM-41 skeleton based on Kinetic Monte Carlo methods. The effect of surface groups and gas diffusion on MCM-41 was studied using the KMC model. As a result, the amorphous silica model is the most suitable model and consists mainly of two types: hexagonal and cubic mesh. However, structural diagnosis of molecular models has rarely been reported. Therefore, it is needed to analyze the structural and morphological properties of the models to verify its validaty.

Chaffee performed a visualization study of possible inoculation sites for aminopropyltrimethoxysilane (APTMS) on a mesoporous silica. The author has calculated surface interactions using geometric constraints and molecular simulations for amine grafting. The APTMS chains were placed in an orderly fashion at the most energetically favorable grafting sites; however, no studies of adsorption were performed.

Schumacher et al. simulated adsorption of CO_2 in amine or phenyl groups functionalized by co-condensation on MCM-41 and no studies were performed on post-condensation. Using the GCMC, they regenerated the condensation together taking into account the organic group directly bound to a silicon atom of the MCM-41. Using a similar approach, Williams et al. functionalized MCM-41 with a series of different organic groups, studying the effect of different grafted groups on the capture of CO_2.

Zhuo et al. MCM-41 was described as a four-hole model with hexagonal super-celled structure. The simulation result was closely compatible with the experimental results.

Pellenq colleagues described MCM-41 as a single pore model and studied Ar adsorption with the GCMC simulation. They compared adsorption and capillary condensation between cylindrical and hexagon pore models and found that both experimental results and adsorption isotherms from different pore forms with each other.

Malfreyt and his colleagues used the model of a single pore. In the coarse grain model/all atoms (CG/AA) model, mesoscopic interaction potential parameters were obtained from the simulation of methanol adsorption isotherm. However, MD studies are limited to the effect caused by amine groups.

Recently, Seaton et al. simulated a series of amine-grained MCM-41 in different species and numbers. They found that grafted amine group enhanced the adsorption of CO_2 and the selectivity of CO_2/N_2.

3. SIMULATION METHOD

Our simulation method has consisted of three steps:

3.1. Modeling of AP/MCM-41:

Here, our first aim is to obtain a model of aminopropyl-functional MCM-41 structure. The procedure was proceeded in the following way;

1) The repeating unit cell of MCM-41 (crystalline SiO_2) was obtained from Cambridge Cluster Database (CCD)
2) Intended size of MCM-41 was obtained from repeating the unit cell of SiO_2 crystal in Materials Studio Program
3) Aminopropyl bind to the pore surface in a predetermined to match the concentration of aminopropyl.
4) AP/MCM-41 structure was geometrically optimized with Materials Studio program.

The atomic structure of AP/MCM-41 prepared according to the above items was formed as shown Figure 3.1 by repeating 1 unit of cells to the dimensions of 13.511 Å x 9.953 Å x 32.849 Å.

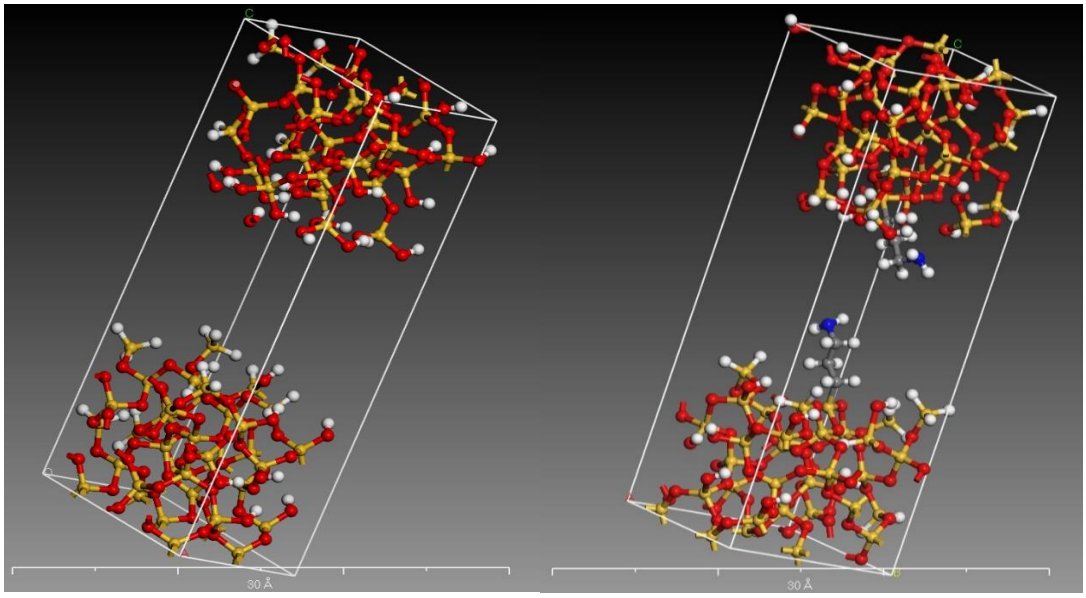

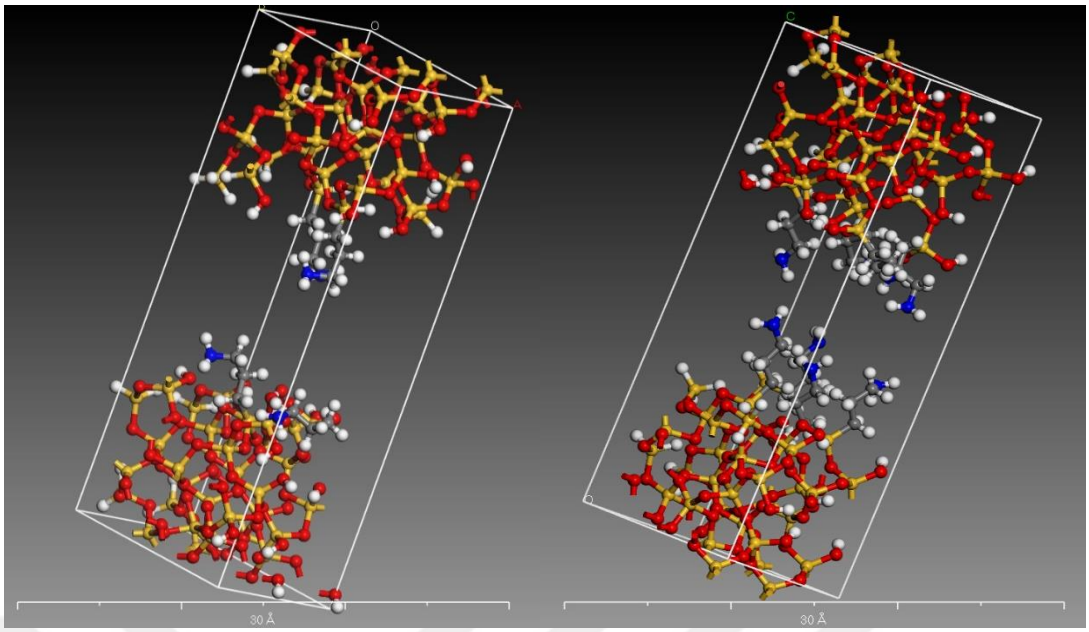

Figure 3.1. Modeling of MCM-41 with different AP loadings. Key: Si, yellow; O, red; H, white; C, gray; N, blue

Table 1: Structural properties of the AP/MCM-41 model

Propeties	**Silica Model**
Cell parameters (Å)	(13.511, 9.953, 32.849)
Lattice angle (º)	(90, 90, 90)
Cell volume (Å³)	4417
No. of Si atoms	66
No. of O atoms	132
No. of H atoms	36
No. of C atoms	12
No. of N atoms	4
Connolly surface area (Å²) (for AP4)	523.65

3.2. Computational Method and Parameters

Interatomic interaction potentials (Van der Waals interactions, Coulombic interaction, bonding, angular and torsion potentials) will be used in geometric optimization and GCMC calculations.

And graphs of approximate functions of these potentials are shown Figure 3.2.

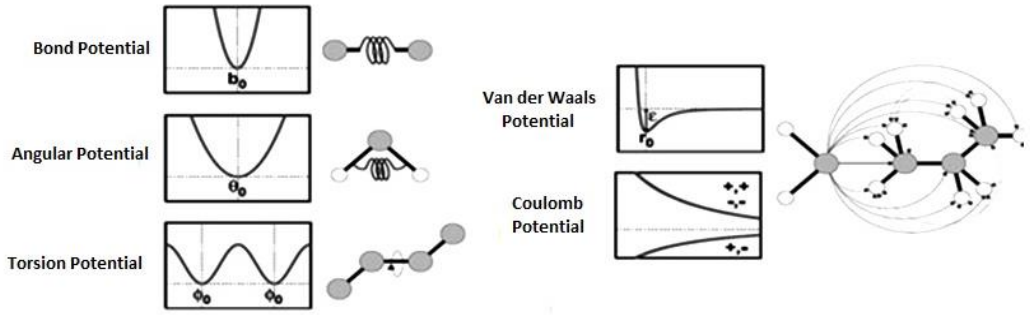

Figure 3.2. Interaction potentials to be used in geometric optimization and in GCMC

We used for system optimization and simulation that the extended potential equation between atoms are as Equation 1.

$$U = \sum_i \sum_{j>i} 4\varepsilon_{ij}\left[\left(\frac{\sigma_{ij}}{r_{ij}}\right)^{12} - \left(\frac{\sigma_{ij}}{r_{ij}}\right)^{6}\right] + \sum_i \sum_{i>j} \frac{q_i q_j}{4\pi\varepsilon_0 r_{ij}} + \sum_i \frac{k_i^{bond}}{2}\left(r_i - r_{0,i}\right)^2 + \sum_i \frac{k_i^{angle}}{2}\left(\theta_i - \theta_{0,i}^{eq}\right)^2 + \sum C_1\left(1 + \cos(\emptyset)\right) + C_2\left(1 - \cos(2\emptyset)\right) + C_3\left(1 + \cos(3\emptyset)\right)$$

Eqn.1

where r_{ij} is the distance between points i and j; ε_{ij} and σ_{ij} are the LJ parameters; q_i is the point charge of i; ε_0 is the vacuum permittivity; k_i^{angle}, θ_i, and θ_i^{eq} are the bending constant, the bending angle, and the equilibrium bending angle respectively; ϕ is the current dihedral angle and C_i (C_1, C_2, C_3) are constant parameters (Builes and Vega, 2012).

3.3. Quantum Mechanical Modeling:

In general, quantum mechanical models produce more complicated and more realistic potential energy surfaces than molecular mechanics models. Most theories in classical physics can be derived from quantum mechanics as an approximation valid at large (macroscopic) scale. Quantum mechanics is essential to understanding the behavior of systems at atomic length scales and smaller. Quantum mechanics was initially developed to provide a better explanation and description of the atom, especially the differences in the spectra of light emitted by different isotopes of the same chemical element, as well as subatomic particles. In short, the quantum-mechanical atomic

model has succeeded spectacularly in the realm where classical mechanics and electromagnetism does not succeed.

Partial charges were found by the help of Materials Studio program by quantum mechanical modeling. The atomic partial charge of these molecular sequences were calculated in the Materials Studio program using the Mulliken population analysis method, Hirshfeld method and ESP-fitted method.

3.4. Surface Area Calculations:

The contact surface is created when a spherical probe (representing the solvent) is rolled over the molecular model. The accessible surface area is calculated from a simple Monte Carlo integration technique where the probe molecule is "rolled" over the framework surface. For this a probe molecule is randomly inserted around each of the framework atoms in turn and checked for overlap with other framework atoms. The fraction of the probe molecules that does not overlap with other framework atoms is then used to calculate the accessible surface area. Conceptually, roll a probe sphere over the molecule. Everywhere the center of the sphere goes is Solvent Accessible Surface; everywhere sphere touches (including empty space) is the Connolly Surface. The surface area of an atom is Van der Walls Surface (See Figure 3.3).

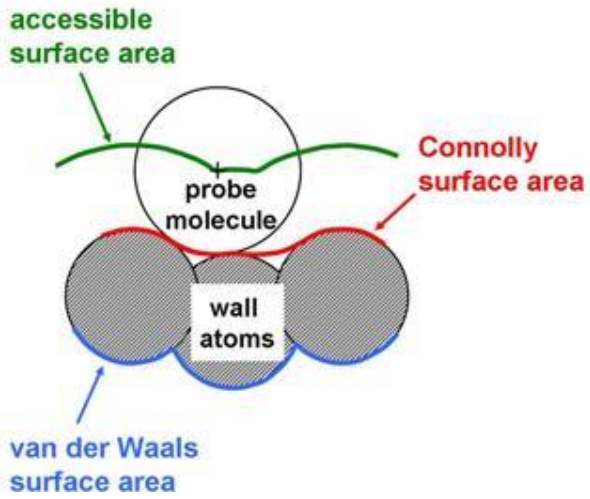

Figure 3.3. Representing Connolly, Accessible and Van der Waals surface area (Duren et al, 2007)

3.5. Reaction Mechanism

The interaction between basic surface functional groups, generally amino groups, and CO_2 molecules, explains the CO_2 capture with these adsorbents, as presented in Figure 3.4. According to this mechanism, the maximum achievable CO_2/N molar ratio value is 0.5 under dry conditions and 1.0 in presence of moisture (Perez et al, 2013). The molar CO_2 adsorption capacity per mol of nitrogen (mol CO_2/mol N) is often considered as a measure of the adsorbent efficiency in the adsorption process.

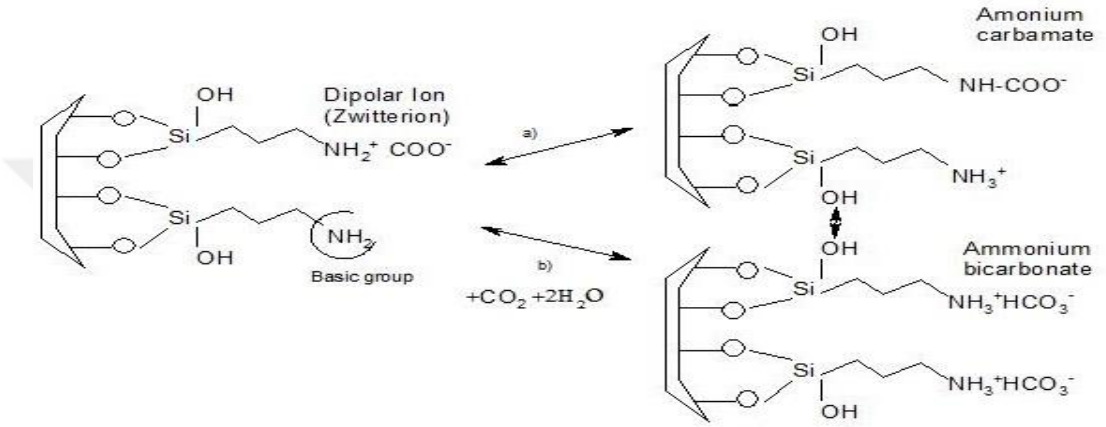

Figure 3.4. Sequence of reactions performed by AP/MCM-41 with CO_2 (Perez et al, 2013)

3.6. GCMC (Grand Canonical Monte Carlo) Simulation:

Forcefield parameters of AP/MCM-41 will be used as input data in a specially written RASPA simulation program for simulations which is open source and prepared for simulation of adsorption processes of porous materials. Adsorption isotherms and adsorption enthalpy values of each of the different models obtained by grafting different loadings of AP groups obtained by GCMC simulation technique.

3.6.1. AP concentration effect

- Models prepared at different AP concentrations (3.5%, 4.2% and 5.2%) used to determine CO_2 adsorption capacities in MCM-41 sorbent by GCMC simulations at different temperatures and pressures.
- The surface bonding energies and isothermal curves obtained for these different AP loads will be compared with the experimental data in the literature.

Weight percentage of Connolly surface area calculations are calculated as follows;

$$\text{Weight Percentage (\%) of AP Loading} = \frac{\text{Surface AP2} - \text{Surface AP0}}{\text{Surface AP0}}$$

CSA_{AP0}= 100.15 Å^2
CSA_{AP2}= 450.82 Å^2
CSA_{AP4}=523.65 Å^2 CSA_{AP8}=623.53 Å^2

$$\text{AP2 \%} = \frac{450.82-100.15}{100.15} = 3.501\ \%$$

$$\text{AP4\%} = \frac{523.65-100.15}{100.15} = 4.228\ \%$$

$$\text{AP8\%} = \frac{623.53-100.15}{100.15} = 5.225\ \%$$

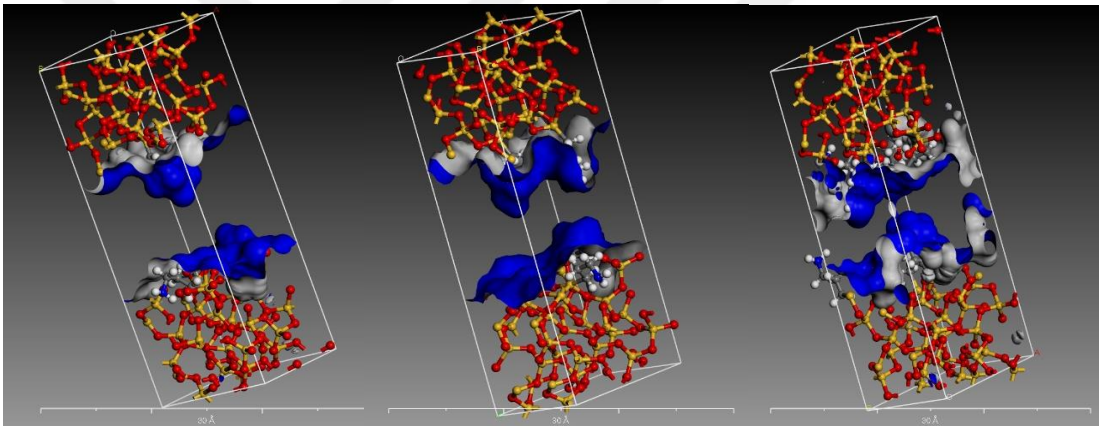

Figure 3.5. AP2, AP4, AP8 Connolly Surface Area of depiction on Materials Studio program

3.6.2. Effect of N_2 to CO_2 adsorption processes

The planned tasks to understand the SO_2 effect in the CO_2 adsorption process are given below, respectively.

- To decrease the simulation time, the atomic partial charge and Van der Waals energies are calculated.
- Adsorption isotherm curves will be obtained from two different mixture media (100% CO_2 + 25% N_2 and 75% CO_2 + 25% N_2).

3.6.3. The impact of H_2O to CO_2 and SO_2 adsorption processes

- Analysis of SO_2 adsorption capacity in H_2O environment, it has been observed in some studies that SO_2 adsorption increased at 25% humidity, and remained the same in a humidity-free environment and 100% humidity environment.
- In this study, we also performed the H_2O (1 %, 2%, 3%) and SO_2 (0.1%, 1%, 10%) loads at different rates and calculate the individual adsorption capacities and total adsorption capacity for each gas with a detailed analysis and we examined the influence of AP/MCM-41 sorbent on CO_2 adsorption capacity of the environmental humidity.

4. RESULTS AND DISCUSSION

4.1. Effect of AP Concentration on CO_2 Adsorption

Different AP concentrations (3.5 %, 4.2 % and 5.2 %) are used to determine CO_2 adsorption capacities in MCM-41 sorbent. Figure 4.1 show that adsorption capacity decreases as the AP concentration increases. The difference in adsorption capacity between AP0 and AP2 appears to be 0.5 loadings per cell, difference in adsorption capacity between AP0 and AP4 appears to be 0.2 loadings per cell and than difference in adsorption capacity between AP0 and AP8 appears to be 3 loadings per cell. At low pressures no change of occured to about 3000 kPa. While the adsorption capacity of AP0, AP2, AP4 are the same at 5000 kPa which is 6 loadings per cell; the adsorption capacity of the AP8 is about 4.2 loadings per cell. We will then took AP4 as a reference and perform the calculations over it, because iy has the highest CO_2 adsorption.

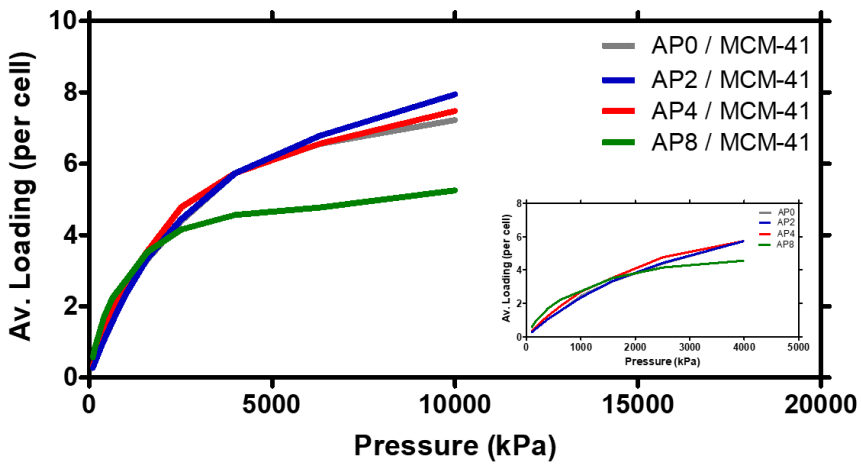

Figure 4.1. Adsorption isotherm curves of different AP loading on MCM-41

4.2. Effect of flue gas N_2 on CO_2 Adsorption

Although no change is observed at low pressures, adsorption capacity was decreased at medium pressures with N_2 but becomes stable afterwards. A small fluctuation is observed at high pressures. N_2 in Flue gas was observed not to affect adsorption capacity much it is seen in Figure 4.2. Adsorption capacity at different CO_2 concentrations was about 6 loadings per cell at 5000 kPa, while a fluctuation between 5000 to 10000 kPa occurred.

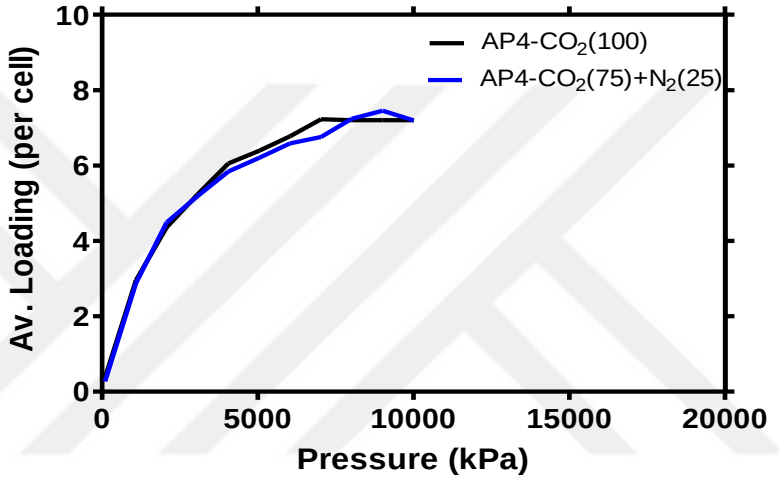

Figure 4.2. Adsorption isotherm curves of AP/MCM-41 with CO_2 (100%) and CO_2+N_2 (75%+25%)

When comparing different CO_2 concentrations, no change of up to 5000 kPa was observed. The adsorption capacity of 5000 kPa is again 6 loadings per cell. Then a fluctuation was observed again in the Figure 4.3. at higher pressures no change was observed up to 5000 kPa.

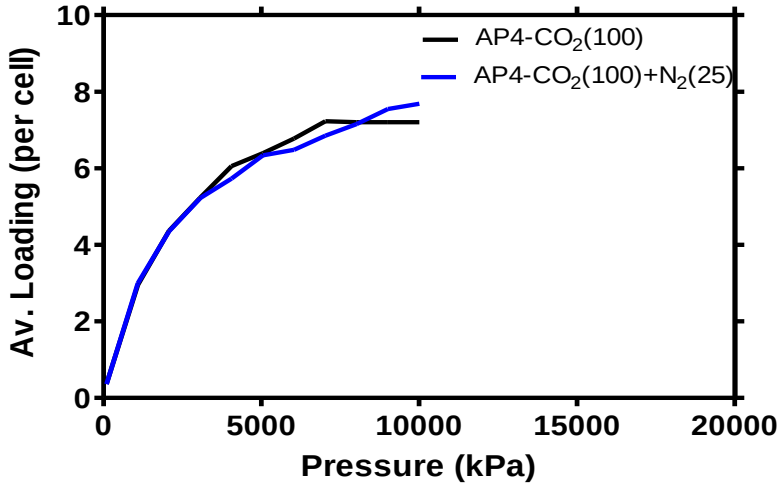

Figure 4.3. Adsorption isotherm curves of AP/MCM-41 with CO_2 (100%) and CO_2+N_2 (100%+25%)

4.3. Atomic Partial Charges of Aminopropyl+SiO_2

Atomic partial charges of all the atoms in AP/CM-41 which are calculated by different methods with Materials Studio program. These values are compared in Table 2.

Table 2. Comparison of atomic partial charges by different method

Elements Type	Hirshfeld Method	Mulliken Method	ESP-fitted Charges
C_1	-0.1274	-0.783	-0.794
C_2	-0.0522	-0.397	0.229
C_3	-0.0100	-0.224	0.282
N	-0.2374	-0.784	-1.025
H_1	0.0324	0.221	0.163
H_2	0.0315	0.227	0.177
H_3	0.0305	0.217	0.009
H_4	0.0278	0.218	0.001
H_5	0.0155	0.176	-0.035
H_6	0.0340	0.198	0.044
H_7	0.0986	0.318	0.353
H_8	0.0988	0.321	0.367
Si	0.5179	1.338	1.079
O_1	-0.3677	-0.893	-0.747
O_2	-0.3437	-0.886	-0.724
H_9	-0.0596	-0.112	-0.150
H_{10}	0.1522	0.416	0.365
H_{11}	0.1602	0.427	0.406

The comparison of atomic partial charges of propylamine (PA), ethylamine (EA) and methylamine (MA) of different amine groups is shown in Table 3.

Table 3. Comparison between Amines group atomic partial charges;

Element Type	Propylamine (PA, C_3H_9N)	Ethylamine (EA, $C_2H_5NH_2$)	Methylamine (MA, CH_3NH_2)
N	-1.025	-0.973	-0.882
H_N	-0.150	-0.155	-0.115
C_1	-0.794	-0.018	-0.216
C_2	0.229	0.245	
C_3	0.282		
H_1	0.177		
H_2	0.009		

4.4. Effect of H_2O on CO_2 Adsorption

No change in low pressures, up to 3000 kPa, was observed in the CO_2 adsorption capacity of AP/MCM-41 sorbent in the presence of H_2O at 1%, 2% and 3%. After 3000 kPa, a fluctuation was observed in all three ratios. In the Figure 4.4, it is observed that there is not much change in the adsorption value of CO_2 in the presence of H_2O at low pressure. While value is 6 loadings per cell in all three ratios at 6000 kPa, and then increases to about 7 loadings per cell at 10000 kPa.

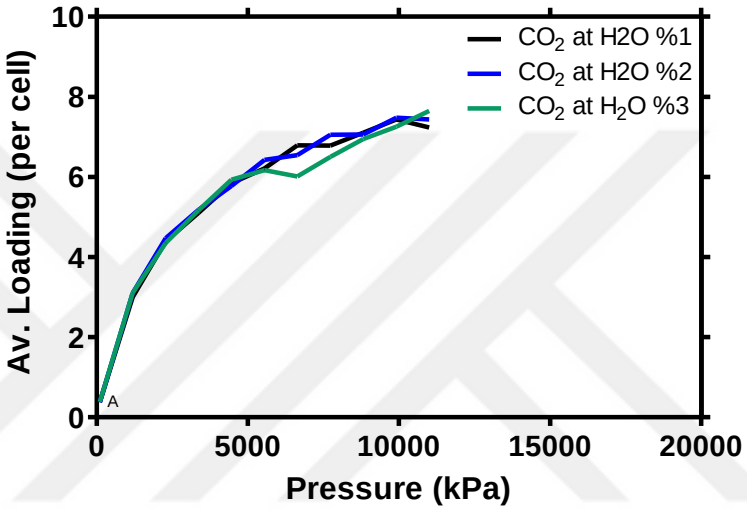

Figure 4.4. Adsorption isotherm of CO_2 adsorption with H_2O (1%, 2%, 3%) on AP/MCM-41

Very little changes have been observed in the adsorption energies as well as the absorption capacities. Adsorption energy of CO_2 is around 2 kcal/mol in all three H_2O loads in the Figure 4.5.

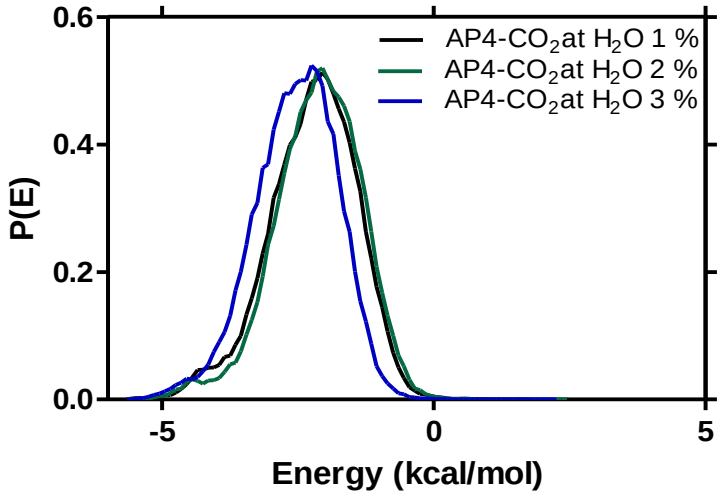

Figure 4.5. Adsorption energy values of CO_2 at different H_2O loading (1%, 2%, 3%)

4.5. Effect of SO_2 on CO_2 Adsorption

In the AP/MCM-41 sorbent, 0.1%, 1% and 10% SO_2 loadings were performed and no apparent effect was observed on adsorption capacity, especially at low pressures. Adsorption was 2.3 loadings per cell from 4000 kPa to 7000 kPa, slightly fluctuating in the Figure 4.6. At the inset figure in the Figure 4.6, adsorption isotherm of AP/MCM-41 with SO_2 (0.1%, 1 %, 10 %), it is observed that there is not much change in the adsorption value of CO_2 in the presence of SO_2.

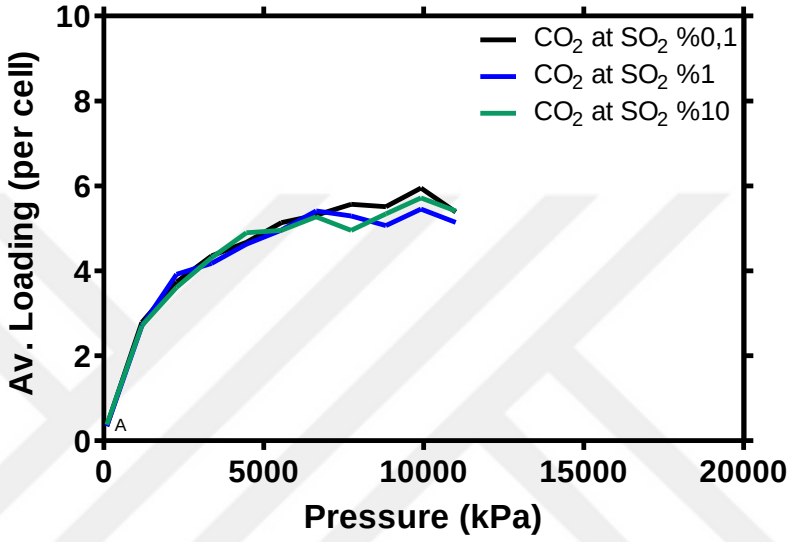

Figure 4.6. Adsorption isotherm of CO_2 with SO_2 (0.1%, 1 %, 10 %) on AP/MCM/41

The adsorption energies of CO_2 gave different results in all three SO_2 loading. Energy values of about 3 kcal/mol was observed at 0.1% SO_2 loadings; 2.5 kcal/mol at 1% SO_2 loading and about 5 kcal/mol at 10% SO_2 loading in the Figure 4.7.

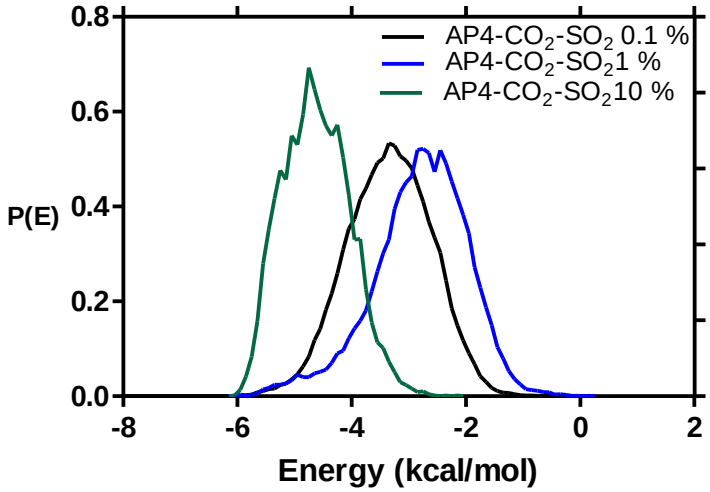

Figure 4.7. Adsorption energy values of CO_2 at different SO_2 loading (0.1%, 1%, 10%)

4.6. Effect of Temperature on CO_2 Adsorption

Adsorption capacity was obtained at different AP loads (AP2, AP4, AP8) and at different temperatures (298 K, 348 K and 398 K), and it was observed as the temperature is increased, the adsorption capacity decreased in the Figure 4.8. Adsorption capacity was observed 0.8 loadings per cell at 398 K, 1.5 loadings per cell at 348 K, 2.5 loadings per cell at 298 K at 5000 kPa.

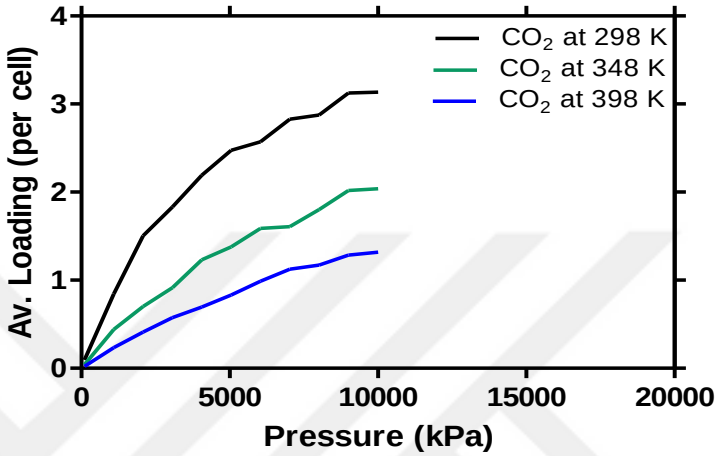

Figure 4.8. Comparison of Temperature effect of CO_2 adsorption on AP/MCM-41

In energy comparisons at different temperatures, it was observed that energy values sligth is decreased as temperature is increased in the Figure 4.9. It was seen as 3.75 kcal/mol at 298 K, 3.0 kcal/mol at 348 K and 2.5 kcal/mol at 398 K.

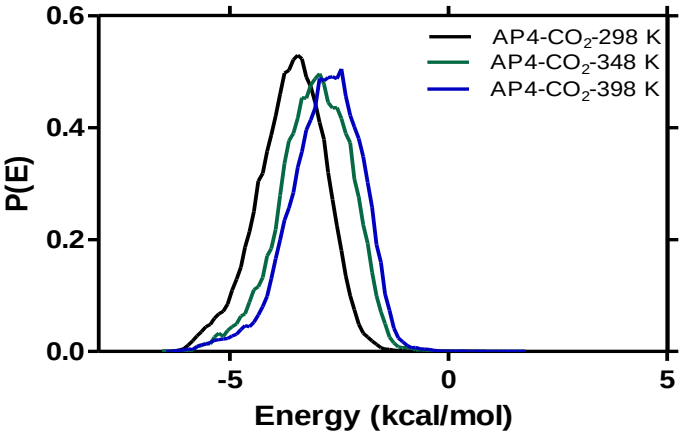

Figure 4.9. Adsorption energy values of CO_2 adsorption at different temperature (298K, 348K, 398K) on AP/MCM-41

5. CONCLUSIONS

In this thesis, adsorption isotherm and adsorption energy of CO_2 on AP/MCM-41 were investigated using Grand Canonical Monte Carlo simulation method. The most average concentration of AP, which is AP4, was selected and calculations were made on AP4.

In the presence of N_2, there was no change in the CO_2 adsorption at low pressures and there was slight fluctuations at high pressures.

Comparing the different amine groups, the atomic charges of propylamine were higher than the others (ethylamine and methylamine).

In the same way, the adsorption of CO_2 was calculated in the presence of SO_2 and H_2O, which did not show much contribution to the CO_2 adsorption on AP/MCM-41.

In the calculations made at different temperatures, it was observed that the adsorption capacity of CO_2 decreases as the temperature increases and the adsorption energy of CO_2 decreases in the same way.

We modelled a MCM-41 model and geometric optimization was performed. Increasing temperature and pressure were a dominant factors for adsorptions. We compared that adsorption was also inversely proportional to the ESP charges (AP, EP, MP). As a result, AP4 had high adsorption capacity.

Population analysis can be performed on the molecular system. The areas where CO_2 is fully located can be detected. In this way, more data and higher accuracy can be obtained. For different situations, a two-dimensional map of AP/MCM-41 can be obtained so that the active sites, where the concentration of CO_2 and N_2 in the pores, can be examined more thoroughly.

6. REFERENCES

Alothman, Z.A. 2012. A Review: Fundamental Aspects of Silicate Mesoporous Materials. 12:5, 2874-2902.

Anonymous, 2019. MCM-41 Synthesis. https://en.wikipedia.org/wiki/MCM-41. (Date of access:06.03.2019)

Balas, F., Manzano, M., Horcajada, P. and Vallet-Regí, M. 2006. Confinement and controlled release of bisphosphonates on ordered mesoporous silica-based materials. *J. American Chemical Society*. 128 8116-8117.

Beck, J.S., Vartuli, J.C., Roth, W.J., Leonowicz, M.E., Kresge, C.T., Schmitt, K.D. Chu, C., Olson, D.H., Sheppard, E.W., McCullen, S.B., Higgins, J.B. and Schlenker, J.L. 1992. A new family of mesoporous molecular sieves prepared with liquid crystal templates. *J. Am. Chem. Soc*. 114, 10834–10843.

Berggren, A., Palmqvist A.E.C., Holmberg K. 2005. Surfactant-templated mesostructured materials from inorganic silica. *Soft Matter*, 1:3, 219-226.

Cao, D.P., Shen, Z.G., Chen, J.F., Zhang, X.R. 2004. Experiment, molecular simulation and density functional theory for investigation of fluid confined in MCM-41. *Microporous Mesoporous Mater*, 67, 159–166.

Che, S., Liu, Z., Ohsuna, T., Sakamoto, K., Terasaki, O. and Tatsumi, T. 2004. Synthesis and characterization of chiral mesoporous silica. *Nature*, 429, 281-284.

Che, S., Sakamoto, Y., Terasaki, O., Tatsumi, T. 2001. Control of crystal morphology of SBA-1 mesoporous silica. *Chemical Materials*, 13(7), 2237-2239.

Chempath, S., Duren, T., Sarkisov, L. and Snurr, R.Q. 2013. Experiences with the publicly available multipurpose simulation code, Music Molecular Simulation. 2013;39:1223–1232. doi:10.1080/08927022.2013.819103.

Ciesla, U. and Schüth, F. 1999. Ordered mesoporous materials ; Microporous and Mesoporous Materials 27, 131-149

Coasne, B., Di Renzo, F., Galarneau, A., Pellenq, R.J.M. 2008. Adsorption of simple fluid on silica surface and nanopore: effect of surface chemistry and pore shape, *Langmuir* 24 7285−7293.

Coasne B., Galarneau A., Di Renzo F., Pellenq R., Gas adsorption in mesoporous micelle-templated silicas: MCM-41, MCM-48, and SBA-15. 2006. *Langmuir* 22, 11097–11105.

Corma, A., Fornés, V., Navarro, M.T., Pérez-Patiente, J. 1994. Acidity and stability of MCM-41 crystalline aluminosilicates. *Journal Catalysis*, 148(2), 569-574.

Diaz, J.F., Balkus, K.J.Jr.1996. Enzyme immobilization in MCM-41 molecular sieve. Journal Molecular Catalysis B: Enzymatic. 2(2-3), 115-126.161

Ding, L.F., Yazaydin, A.O. 2013. The effect of SO_2 on CO_2 capture in zeolitic imidazolate frameworks. *Physical Chemistry Chemical Physics*, vol. 15, no. 28, 11856–11861.

Dos Santos, T. C.; Bourrelly, S.; Llewellyn, P. L.; de M. Carneiro, J. W.; Machado Ronconi, C. Adsorption of CO2 on Amine-Functionalised MCM-41: Experimental and Theoretical Studies. *Phys. Chem. Chem. Phys*. 2015, 17, 11095−11102.

Feng, X., Fryxell, G.E., Wang, L-Q, Kim, A.Y., Liu, J., Kemner, K.M. 1997. Functionalized Monolayers on Ordered Mesoporous Supports. *Science*, 276(5314), 923-926.

Feuston, B.P., Higgins, J.B., 1994. Model structures for MCM-41 materials: a molecular dynamics simulation. *J. Phys. Chem*. 98, 4459–4462.

Garcia-Bennett, A.E., Terasaki, O., Che, S., Tatsumi, T. 2004. Structural investigations of AMS-n mesoporous materials by transmission electron microscopy. *Chemical Materials*, 16: 813- 821.

Ghoufi, A., Morineau, D., Lefort, R., Malfreyt P.2008. Toward a coarse graining/all adsorption of CO_2, N_2 and flue gas in a mimetic MCM-41. *J. Phys. Chem*. C 112, 11295–11300.

Grün, M., Kurganoz, A.A., Schacht, S., Schütz, F., Unger, K.K. 1996. Comparison of an ordered mesoporous aluminosilicate, silica, alumina, titania and zirconia in normalphase high-performance liquid chromatography. *Journal of Chromatography*, 740, 1-9.

Gupta, A., Chempath, S., Sanborn, M.J., Clark, L.A., Snurr, R.Q. 2003. Objectoriented programming paradigms for molecular modeling. Molecular Simulation. 29:29–46. doi:10.1080/0892702031000065719.

Gusev, V.Y., Feng, X., Bu, Z., Haller, G.L., O'Brien, J.A. 1996. Mechanical Stability of Pure Silica Mesoporous MCM-41 by Nitrogen Adsorption and Small-Angle X-ray Diffraction Measurements. *Journal of Physical Chemistry*, 100:6, 1985-1988.

Güçbilmez, Y. 2005. Vanadium and Molybdenum Incorporated MCM-41 Catalysts for Selective Oxidation of Ethanol, Master Thesis, METU.

He, Y.F., Seaton, N.A. 2003. Experimental and computer simulation studies of the adsorption of ethane, carbon dioxide, and their binary mixtures in MCM-41. *Langmuir* 19, 10132‑10138.

Hoffmann, F., Cornelius, M., Morell, J., Fröba, M. 2006. Silica-based Mesoporous Organic-Inorganic Hybrid Materials. Angew. *Chem. Int. Ed*, 45, 3216-3251

Huo, Q., Leon, R., Petroff, P.M., Stucky, G.D.1995. Mesostructure design with gemini surfactants: supercage formation in a three-dimensional hexagonal array. *Science*, 268(5215), 1324-1327.

Ho, N.L., Pellitero, J.P., Porcheron, F., Pellenq, R. 2012. Enhanced CO_2 Solubility in Hybrid Adsorbents: Optimization of Solid Support and Solvent Properties for CO_2 Capture. *J. Phys. Chem*. C201211653600-3607.

Igarashi, N., Tanaka, Y., Nakata, S., Tatsumi, T. 1999. Increased stability of organically modified MCM-41 synthesized by a one-step procedure. *Chemical Letters*, 1, 1-2.

Jing, Y., Wei, L., Wang, Y.D., Yu, Y.X. 2013. Molecular simulation of MCM-41: Structural properties and adsorption of CO_2, N_2 and flue gas. *Chemical Engineering Journal*, vol. 220, 264–275.

Kim, J.M., Kim, S.K., Ryoo, R.1998. Synthesis of MCM-48 single crystals. *Chemical Communications*, 259- 260.

Kim, S.S., Zhang, W., Pinnavaia, T.J. 1998. Ultrastable Mesostructured Silica Vesicles. *Science*, 282(5392), 1302-1305.

Kisler, J.M., Gee, M.L., Stevens, G.W., O'Connor, A.J. 2003. Comparative study of silylation methods to improve the stability of silicate MCM-41 in aqueous solutions. *Chemical Materials*, 15:3, 619-624.

Kleestorfer, K., Vinek, H., Jentys, A. 2001. Structure simulation of MCM-41 type materials. *J. Mol. Catal. A Chem*., 166 :2001, 53–57.

Koh, C.A., Montanari, T., Nooney, R.I., Tahir, S.F., Westacott, R.E. 2011. Experimental and Carbon dioxide capture-related gas adsorption and separation

in metal-organic frameworks. *Coordination Chemistry Reviews*, 255, 1791-1823.

Konstantakou, M., Gotzias, A., Kainourgiakis, M., K. Stubos, A. And A. Steriotis, T. 2011. GCMC Simulations of Gas Adsorption in Carbon Pore Structures. *National Center for Scientific Research Demokritos*, 214, 653-676.

Kresge, C.T., Leonowics, M.E., Roth, W.J., Vartulli, J.C., Beck, J.S. 1992. Ordered mesoporous molecular sieves synthesized by a liquid-crystal template mechanism. *Nature*, 359:6397, 710-712.

Kuchta, B., Llewellyn, P., Denoyel, R., Firlej, L. 2004. Modeling of pore wall amorphous structures: influence of wall heterogeneity on the mechanism of adsorption krypton and argon adsorption in MCM-41 pore model. *Colloids Surf*. A 241,137–142.

Landau, M.V., Varkey, S.P., Herskowitz, M., Regev, O., Pevzner, S., Sen, T., Luz, Z.1999. Wetting stability of Si-MCM-41 mesoporous material in neutral, acidic and basic aqueous solutions. *Microporous Mesoporous Matererials*, 33:1-3, 149-163.

Lim, M.H. 1999. Stein A. Comparative Studies of Grafting and Direct Syntheses of Inorganic-Organic Hybrid Mesoporous Materials. *Chemical Materials*, 11:11, 3285-3295.

Llewellyn, P.L., Ciesla, U., Decher, H., Stadler, R., Schueth, F., Unger, K.K. 1994. MCM-41 and Related Materials as Media for Controlled Polymerization Processes. *Study of Surface Science Catalysis*, 84, 2013-2020.

Long, J.R., Yaghi, O,M. 2009. The pervasive chemistry of metal-organic frameworks. *Chemical Society Reviews*. 38:1213–1214. doi:10.1039/b903811f.

Melo, R.A.A., Giotto, M.V., Rocha, J., Gonzalez, E.A. 1999. MCM-41 ordered mesoporous molecular sieves synthesis and characterization. *Materials Research*, 2, 173-179.

Mercier, L., Pinnavaia, T.J. 1997. Access in mesoporous materials. Advantages of a uniform pore structure in the design of a heavy metal ion adsorbent for environmental remediation. *Advanced Materials*, 9:6, 500-503.

Moller, K. and Bein, T. 1998. Inclusion Chemistry in Periodic Mesoporous Hosts. *Chemical Mater*. doi:199810102950-2963.

Namba, S,. Mochizuki, A., Kito, M. 1998. Fine control of pore size of highly ordered MCM-41 by using template mixtures of dodecyltrimethylammonium bromide/ hexadecyl trimethyl-ammonium bromide with various molar ratios. *Chemical Letters*, 569- 570.

Namba, S., Mochizuki, A., Kito, M. 1998. Preparation of highly ordered MCM-41 with docosyltrimethylammonium chloride (C22TMAC1) as a template and fine control of its pore size. *Studies in Surface Science Catalysis*, 117, 257- 264.

Ohkubo, T., Ogura, T., Sakai, H., Abe, M. 2007. Phase behaviour of cationiv and anionic mixed surfactant. *J Colloid Interf Sci*, 312: 42

Olson, D.H., Sheppard, E.W., McCullen. S.B., Higgings, J.B., Schlenker, J.L.1992. A new family of mesoporous molecular sieves prepared with liquid crystal templates. *Journal of American Chemical Society, 114*:27, 10834-10843.

Pera-Titus, M. 2014. Porous Inorganic Membranes for CO_2 Capture: Present and Prospects. *Chemical Reviews*, 114 :2, 1413–1492.

Prouzet, E., Pinnavaia, T.J. 1997. Assembly of mesoporous molecular sieves containing wormhole motifs by a nonionic surfactant pathway: control of pore size by synthesis temperature. Angewandte Chemie International Edition, 36:5, 516-518.

Raimondo, M., Perez, G., Sinibaldi, M., De Stefanis, A., Tomlinson, A.A.G.1997. Mesoporous M41S materials in capillary gas chromatography. *Chemical Communications*, 15, 1343-1344.

Ravikovitch, P. I., Domhnaill, S.C.O., Neimark, A.V., Schuth, F., Unger, K.K. 1995. Capillary Hysteresis in Nanopores: Theoretical and Experimental Studies of Nitrogen Adsorption on MCM-41, *Langmuir*, 11, 4765.

Ribeiro Carrott, M.M.L., Estevao Candeias, A.J., Carrott, P.J.M., Unger, K.K. 1999. Evaluation of the Stability of Pure Silica MCM-41 toward Water Vapor. *Langmuir 15*:26, 8895-8901.

Roth, W.J. and Vartuli, J.R. 2005. Synthesis of mesoporous molecular sieves. Studies in Surface Science and Catalysis 157, 91-110.

Ryoo, R. and Jun, S. 1997. Improvement of Hydrothermal Stability of MCM-41 Using Salt Effects during the Crystallization Process. *Journal Physical Chemistry*, 101:3, 317-320.

Ryoo, R., Joo, S.H., Kim, J.M. 1999. Energetically favored formation of MCM-48 from cationic-neutral surfactant mixtures. *The Journal Physical Chemistry* B 103, 7435- 7440.

Sakamoto, Y., Kaneda, M., Terasaki, O., Zhao, D., Kim, J.M., Stucky, G.D., Shin, H.J., Ryoo, R.2000. Direct imaging of the pores and cages of three-dimensional mesoporous materials. *Nature*, 408:6811, 449-453.

Sanz-Perez, E.S., Olivares-Marin, M., Arencibia, A., Sanz, R., Calleja, G., Maroto-Valer, M.M. 2013. CO_2 adsorption performance of amino-functionalized SBA-15 under post-combustion conditions. *International Journal Greenhouse Gas Control*,17, 366–375.

Sayari, A. 1996. Periodic mesoporous materials : synthesis, characterization and potential applications. Recent Advances and New Horizons in Zeolite Science and Technology Studies in Surface Science and Catalysis 102, 1-46

Schwanke, A.J., Balzer, R., Pergher S. 2017. Microporous and Mesoporous Materials from Natural and Inexpensive Sources. *Researchgate*, 2-17, DOI: 10.1007/978-3-319-68255-6_43.

Schmidt-Winkel, P., Lukens, W.W., Yang, P., Margolese, D.I., Lettow, J.S., Ying, J.Y., Stucky, G.D.2000. Microemulsion templating of siliceous mesostructured cellular foams with well-defined ultralarge mesopores. *Chemical Materials*, 12:3, 686-696.

Schumacher, C.J., Gonzalez, P.A., Wright, N.A. 2006. Generation of atomistic models of periodic mesoporous silica by kinetic Monte Carlo simulation of the synthesis of the material, *J. Phys. Chem. B*, 110, 319–333.

Selvam, P., Bhatia, S.K., Sonwane, C.G. 2001. Recent advances in processing and characterization of periodic mesoporous MCM-41 silicate molecular sieves", *Ind. Eng. Chem. Res*., 40:15, 3237-3261

Serre, C., Millange, F., Thouvenot, C., Nogues, M., Marsolier, G., Louer, D., Ferey, G. 2002. Very large breathing effect in the first nanoporous chromium(iii)-based solids. *Journal of the American Chemical Society*. 124, 13519–13526. doi:10.1021/ja0276974

Sierra, L., Lopez, B., Guth, J.L. 2000. Preparation of mesoporous silica particles with controlled morphology from sodium silicate solutions and a non-ionic surfactant at pH values between 2 and 6. *Microporous Mesoporous Materials*, 39:3, 519-527.

Snurr, R.Q., Hupp, J.T., Nguyen, S.T. 2004. Prospects for nanoporous metalorganic materials in advanced separations processes. *AIChE Journal*, 50, 1090–1095. doi:10.1002/aic.10101.

Song, X.D., Wang, S., Hao, C., Qiu, J.S. 2014. Investigation of SO_2 gas adsorption in metal–organic frameworks by molecular simulation. State Key Laboratory of Fine Chemicals, Dalian University of Technology, Dalian 116024.

Stein, A., Melde, B.J., Schroden, R. 2000. Hybrid Inorganic-organic Mesoporous Silicates Nanoscopic Reactors Coming of Age. *Advanced Materials*, 12:19, 1403-1419

Suzuki, K., Kenichi, K., Imai, H. 2004. Synthesis of silica nanoparticles having a well-ordered mesostructure using a double surfactant system. Journal American *Chemical Society*, 126, 462- 463.

Tanev, P.T., Pinnavaia, T. 1996. Mesoporous Silica Molecular Sieves Prepared by Ionic and Neutral Surfactant Templating: A Comparison of Physical Properties. *Journal Chemical Materials*, 8:8, 2068-2079.

Tanev, P.T., Chibwe, M., Pinnavaia, T.J. 1994. Titanium-containing mesoporous molecular sieves for catalytic oxidation of aromatic compounds. *Nature*, 368:6469, 321-323.

Trong, O.D., Zaidi, S.M.J., Kaliaguine, S. 1998. Stability of mesoporous aluminosilicate MCM-41 under vapor treatment, acidic and basic conditions. *Microporous Mesoporous Matererials*, 22:1-3, 211-224.

University of Bristol, 2010. Schol of Chemistry, Molecule of the month. http://www.bris.ac.uk/Depts/Chemistry/MOTM/mcm41/mcm41c.htm (Date of access:16.02.2017)

Valiev, M., Bylaska, E.J., Govind, N., Kowalski, K., Straatsma, T.P., Van Dam, H.J.J., Wang, D., Nieplocha, J., Apra, E., Windus, T.L., De Jong, W.A. 2010. NWChem: A comprehensive and scalable open-source solution for large scale molecular simulations. *Computer Physics Communications*.

Vartuli, J.C., Malek, A., Roth, W.J., Kresge, C.T., McCullen, S.B., 2001. The sorption properties of as-synthesized and calcined MCM-41 and MCM-48, *Microporous and Mesoporous Materials*. 44 :45, 691-695.

Vartuli, J.C., Shih, S.S., Kresge, C.T., Beck, J.S. 1998. Potential Applications for M41S Type Mesoporous Molecular Sieves. *Mesoporous Moleculer Sieves*, Vol. 117.

Williams, J.J., Wiersum, A.D., Seaton, N.A., Duren, T. 2010. Effect of surface group functionalization on the CO_2/N_2 separation properties of MCM-41: a grandcanonical Monte Carlo simulation study. *J. Phys. Chem.* C:114 18538–18547.

Xu, W., Luo, Q., Wang, H., Francesconi L.C., Stark, R.E., Akins, D.L.2003. Polyoxoanion Occluded within Modified MCM-41: Spectroscopy and Structure. *Journal of Physical Chemistry* B, 107:2, 497-501.

Yamamoto, K., Tatsumi, T. 2001. Organic functionalization of mesoporous molecular sieves with Grignard reagents. *Microporous Mesoporous Matererials*, 44:45, 459-464.

Yun, J., Duren, T., Keil, F.J., Seaton, N.A.2002. Adsorption of methane, ethane, and their binary mixtures on MCM-41: experimental evaluation of methods for the prediction of adsorption equilibrium, *Langmuir*, 18, 2693–2701.

Zhao, D., Huo, Q., Feng, J., Chmelka, B., Stucky, G.D. 1998. Nonionic triblock and star diblock copolymer and oligomeric surfactant syntheses of highly ordered,

hydrothermally stable, mesoporous silica structures. *Journal of American Chemical Society*,120:24, 6024-6036.162.

Zhao, D., Yang, P., Huo, Q., Chmelka, B., Stucky, G.D. 1998. Topological constructionof mesoporous materials. *Current Opinion Solid State Materials Science*, 3:1, 111-121.

Zhao, X S., Lu, G Q., Millar, G.J. 1996. Advances in mesoporous molecular sieve MCM-41. *Ind. Eng. Chem. Res.*, 35, 2075-2090.

Zhao, X.S., Audsley, F., Lu, G. 1998. Irreversible Change of Pore Structure of MCM-41 upon Hydration at Room Temperature. *Journal of Physical Chemistry*. B 102:21, 4143-4146.

Zhu, Y.J., Zhou, J.H., Hu, J., Liu, H.L. 2012. The effect of grafted amine group on the adsorption of CO_2 in MCM-41: A molecular simulation. *Catalysis Today*, 194 :1, 53–59.

Zhuo, S.C., Huang, Y.M., Hu, J., Liu, H.L., Hu, Y., Jiang, J.W. 2008. Computer simulation for adsorption of CO_2, N_2 and flue gas in a mimetic MCM-41, *J. Phys. Chem*. C:112, 11295–11300.